Fermi surfaces changes in $La_{1-x}Sm_xB_6$ and $Ce_{1-x}Ca_xB_6$ studied using the de Haas–van Alphen effect and magnetic susceptibility

R. G. Goodrich,[1,*] D. P. Young,[1] N. Harrison,[2] C. Capan,[3] and Z. Fisk[3]
[1]*Department of Physics and Astronomy, Louisiana State University, Baton Rouge, Louisiana 70803, USA*
[2]*National High Magnetic Field Laboratory, Los Alamos National Laboratory, Los Alamos, New Mexico 87545, USA*
[3]*Department of Physics and Astronomy, University of California, Irvine, California 92697, USA*
(Received 5 June 2009; revised manuscript received 29 September 2009; published 2 December 2009)

We have made measurements of the de Haas–van Alphen (dHvA) effect and the magnetic susceptibility of $La_{1-x}Sm_xB_6$ for $x=0$, 0.05, and 0.10 and $Ce_{1-x}Ca_xB_6$ for $x=0$ 0.01, 0.03, and 0.05 in order to see changes in the Fermi surface (FS) volume with doping using lower valence substitutions for La and Ce. The FS volume decrease in $La_{1-x}Sm_xB_6$ is found to be directly proportional to the decrease in the number of electrons contributing to the boron-based conduction band by the decrease in valence of the divalent element. Two overlapping pieces of FS in the same portion of the Brillouin zone are seen to decrease in volume to the extent that they no longer overlap. In the case of $Ce_{1-x}Ca_xB_6$ the combination of increased disorder decreasing the mean-free path due to doping and heavy effective masses results in the damping of the dHvA oscillations and no signals are observed above $x=0.05$. Due to the mixed valence of the Ce atoms the volume decrease is not proportional to the percent valence change. Additional magnetic-susceptibility and magnetization measurements show the changing magnetic phase diagram in $Ce_{1-x}Ca_xB_6$. In the antiferroquadrapolar state of all of the $Ce_{1-x}Ca_xB_6$ samples the near-zero applied field magnetization is seen to increase with decreasing temperature terminating in a transition to the antiferromagnetic state.

DOI: 10.1103/PhysRevB.80.233101 PACS number(s): 71.18.+y, 71.20.−b, 71.30.+h, 75.30.Kz

In a previous paper[1] we have reported the observation of the de Haas–van Alphen (dHvA) effect over a complete series of random alloys, $Ce_{1-x}La_xB_6$, where x was changed across the series in approximately 0.1 steps. In these measurements, except for hybridization of the $4f$ electron in Ce leading to the heavy fermion state, the valence of the substitutions is the same as the host material. As a consequence of this nearly constant valence, the size and shape of the Fermi surface (FS) changes very little but the effective mass of the carriers increases as the Ce concentration is increased. In Fig. 1 the known FS of LaB_6 is shown.[2] As can be seen, the FS consists of a set of six overlapping ellipsoids per Brillouin zone (BZ). Two of the ellipsoids that have extremal cross sections out of the page are not shown but the points of overlap with the others are shown as small circles. The observable orbits are indicated as $\alpha_{1,2}$, α_3, γ, and ε. The $\alpha_{1,2}$ signals always appear much weaker in the overall dHvA signal than the α_3 due to the fact that magnetic breakdown in the ellipsoid overlap is required for these orbits to close. The other two orbits, γ and ε are hole orbits and are due to reflections rather than magnetic breakdown at the points of ellipsoid overlap.

In this Brief Report we report the results of high magnetic field dHvA and low magnetic field magnetization measurements on random alloys of $La_{1-x}D_xB_6$ and $Ce_{1-x}D_xB_6$, where D denotes divalent substitutions for trivalent La or Ce. All of the measurements were performed on single crystals of the rare-earth hexaborides with some of the rare-earth atoms replaced by divalent Sm or Ca, grown from stoichiometric components in molten Al. No visible signs of Al inclusion were evident upon magnification. The measurements reported here were made on small single crystals in the shape of square rods having approximate dimensions of 0.25 mm $\times$0.25 mm$\times$1 mm long. Each of these dimensions was along a $\langle 100 \rangle$, or equivalent, axes of the cubic structure, and the magnetic field was applied along the rod axis. The dHvA magnetization measurements were made between 0 and 60 T at the pulsed field facility of the National High Magnetic Field Laboratory (NHMFL) located at the Los Alamos National Laboratory. The details of the measurement technique previously have been reported.[3] The other low-field ($<$8 T) magnetization measurements were made either at LSU or UC Irvine using physical property measurement system (PPMS) or superconducting quantum interference device systems.

Examples of the Fourier transforms, FTs, of the dHvA

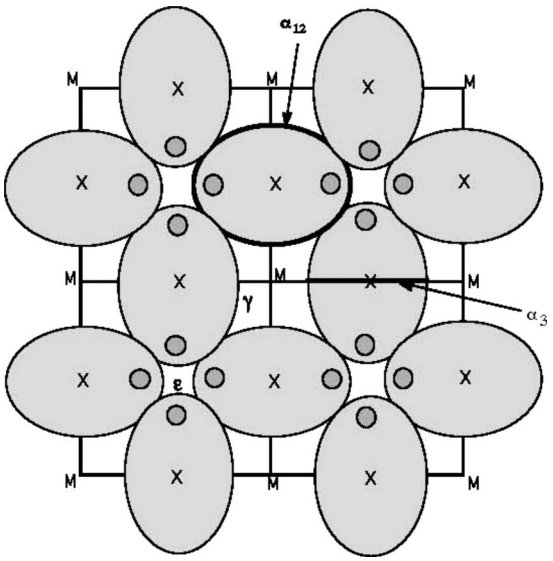

FIG. 1. Fermi Surface of LaB_6 or CeB_6 in the ΓXM plane with the extremal orbits indicated.

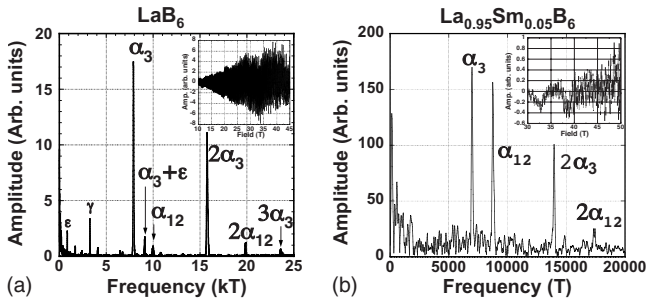

FIG. 2. dHvA frequencies for LaB_6 and $La_{0.95}Sm_{0.05}B_6$ with raw data shown in the insets.

data for LaB_6 and $La_{0.95}Sm_{0.05}B_6$ are shown in Fig. 2. In the $La_{0.9}Sm_{0.1}B_6$ samples the signal-to-noise amplitude ratio approaches one but we have extracted the $\alpha_{1,2}$ and α_3 frequencies by making repeated field sweeps and through averaging the FTs finding which peaks do not change in frequency. All of the orbits indicated in Fig. 1 are present for the LaB_6 data and additional frequencies corresponding to harmonics and sums and differences of frequencies caused by magnetic interactions are observed. In the $La_{0.95}Sm_{0.05}B_6$ data there only are two frequencies and their harmonics corresponding to the $\alpha_{1,2}$ and α_3 orbits slightly shifted in frequency and of much different amplitude ratios from that found in pure LaB_6. In addition the γ and ε frequencies do not rise out of the noise even after repeated sweep averaging. In a previous paper we showed that the FS of LaB_6 and low concentrations of Ce, 1–5 %, in LaB_6 is accurately represented by ellipsoids of revolution.[4] Because the FS is composed of ellipsoids of revolution, the two observed frequencies $\alpha_{1,2}$ and α_3 corresponding to the two extremal areas of the ellipsoid are all that are required to calculate the FS volume and hence the carrier density. Comparing the volume of the FS in $La_{0.95}Sm_{0.05}B_6$ to the FS volume of LaB_6 we find a 5% reduction. In the $La_{0.9}Sm_{0.1}B_6$ there is a 10% reduction. It is interesting to note that in this reduction Sm goes in as a divalent atom, and not mixed valence (see Table I). This result agrees with that of Kasaya, *et al.*[5] for the concentrations studied here. The resulting FSs for these three Sm concentrations are shown in Fig. 3. Only two of the six ellipsoids of revolution centered at X points are shown in each case with the overlap shown expanded on the right.

Because the overlap of the FS ellipsoids begins to become smaller in the 5% Sm sample the magnetic breakdown appears to be total in the field range of measurement in the $La_{0.95}Sm_{0.05}B_6$ sample with no reflections at the points of overlap that form the γ or the ε orbits, giving the α_3 and $\alpha_{1,2}$

TABLE I. $La_{1-x}Sm_xB_6$.

x	α_3 frequency (T)	$\alpha_{1,2}$ frequency (T)	FS volume ($\times 10^{11}$) (cm^{-3})	Percent volume change
0	7895	9973	1.503	0
0.05	7850	9832	1.478	5.07
0.10	7800	9700	1.453	9.96

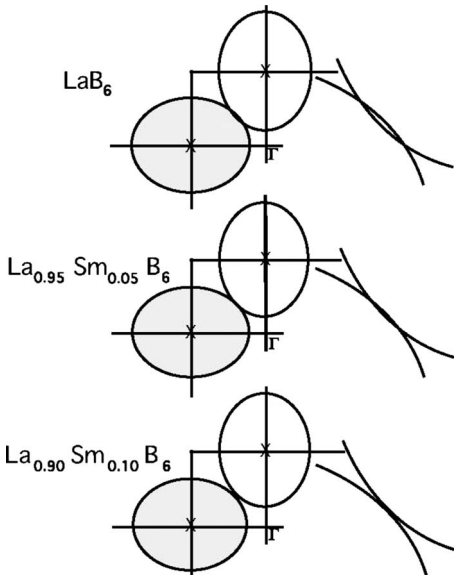

FIG. 3. Cross sections of the ellipsoidal FSs of $La_{1-x}Sm_xB_6$ for various values of x under the assumption that the shape remains constant.

signals almost equal amplitude. Note that in LaB_6, the orbit normally observed from magnetic breakdown ($\alpha_{1,2}$), is much smaller in amplitude than the central smaller orbit (α_3). The lower-frequency large-amplitude peaks in the FT shown in Fig. 2 are the α_3 (ellipsoid a-axis area) and the second $\alpha_{1,2}$ (ellipsoid ab axes area seen in Fig. 1). The next two peaks in Fig. 2 are harmonics of the first two. Other small peaks in the FT of Fig. 2 for LaB_6 are due to magnetic interactions causing sums and differences of the primary frequencies to be observed.

The FS volume can be calculated in the same manner used in our previous work on EuB_6.[3] From the $\alpha_{1,2}$ and α_3 frequencies in Fig. 2 the volume of the FS is obtained from orbit areas using the Onsager relation to obtain the area, $A=(2\pi e/c)F=(9.546\times 10^{11})F$, where A is the extremal cross-sectional area of the FS in $(cm)^{-2}$ and the frequency is measured in kilotesla, kT. For an ellipsoid of revolution, the volume, $V=(4/3)\pi a^2 b$, of the FS is given in terms of areas by $V=(4/3\pi^{1/2})(A_3)^{1/2}A_{1,2}$, where the area corresponding to the α_3 frequency, $A_3=\pi a^2$, is the minimum area of the ellipsoid of revolution, and the area corresponding to the $\alpha_{1,2}$ frequency, $A_{1,2}=\pi ab$, is the maximum area.

In Table I we list the measured $\alpha_{1,2}$ and α_3 frequencies, the calculated volume of the ellipsoid, and the percent volume change for each concentration of divalent metal for $La_{1-x}Sm_xB_6$. For Fig. 3 we determined (a) the minor axis and (b) the major axis from the above equations and then plotted ellipsoids using these radii as fractions of the Γ-X distance in the BZ using the low-temperature lattice constant of Booth, *et al.*[6] In addition we have measured the change in lattice constants for this series of alloys and find that they change less than 0.5% over the range of Sm substitutions measured here. No significant change in the light effective masses of these compounds was observed.

Typical FTs and raw data for CeB_6 and $Ce_{0.95}Ca_{0.05}B_6$ are shown in Fig. 4. For the Ce alloys, to make meaningful com-

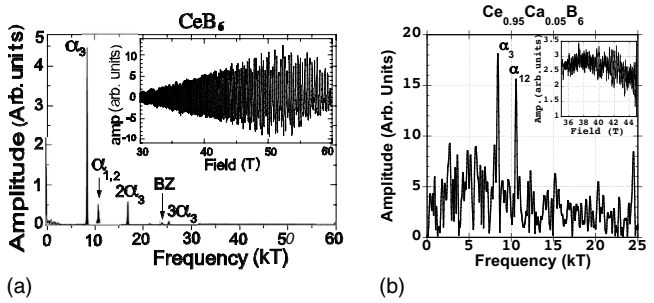

FIG. 4. dHvA frequencies for CeB_6 and $Ce_{1-x}Ca_xB_6$ with raw data shown in the insets.

parisons between their frequencies and the α_3 and α_{12} frequencies of pure CeB_6, one must be careful to make the comparisons with data taken in the same field range because it is known that the frequencies and FS shape are field dependent[7] although the FS volume remains constant as a function of field. The α_3 frequency of CeB_6 in the field range of 40–50 T where the current data analyses were made, given by Haanappel *et al.*,[8] is 8670 T. This previously measured value agrees to better than 1% with the current measured value shown in Table II. Similar to $La_{1-x}Sm_xB_6$, the FS of $Ce_{1-x}Ca_xB_6$ shrinks with increasing Ca concentration. The FS volume changes for the 1% and 3% Ca samples are consistent within experimental error with the % Ca. However, this is not the case for the 5% sample. Here the decrease is over 7% meaning that something besides just replacing trivalent Ce with divalent Ca is occurring. We suggest that the amount of mixed valency is changing and more of the Ce 4*f* electrons are localized in the 5% Ca concentration. Since we were only able to observe signals at the lowest temperature, no temperature dependence was possible to determine the effective mass.

In addition to the dHvA measurements on the $Ce_{1-x}Ca_xB_6$ samples, we have measured the near-zero applied field magnetic susceptibility of several samples with different doping levels. The temperature dependence of the ac susceptibility at 10 Oe for $x=0$, 0.01, 0.03, 0.05, and 0.07 is shown in Fig. 5. Subsequent measurements at the NHMFL of the zero-field susceptibility of a 10% sample to less than 1 K shows a turnover similar to the curves shown in Fig. 5, i.e., the phase II to phase III transition occurs at 0.6 K. As can be seen in the inset the temperature at which the transition from the paramagnetic to antiferroquadrupolar (AFQ) state occurs is reduced with increasing Ca concentration. It is not known why an increase in magnetization, and hence the magnetic

TABLE II. $Ce_{1-x}Ca_xB_6$.

x	α_3 frequency (T)	$\alpha_{1,2}$ frequency (T)	FS volume ($\times 10^{11}$) (cm^{-3})	Percent volume change
0	8620	10600	1.669	0
0.01	8461	10672	1.665	0.76
0.03	8434	10615	1.654	2.83
0.05	8390	10488	1.620	7.15

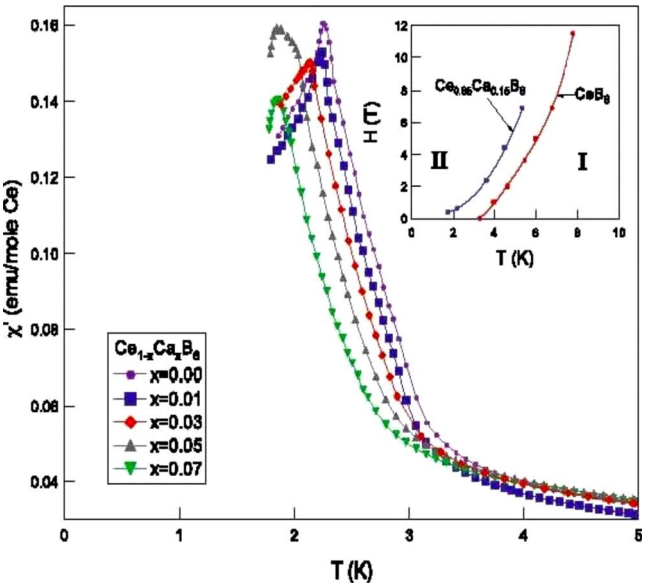

FIG. 5. (Color online) Susceptibility of Ca-doped CeB_6, taken at an applied field of 10 Oe showing the suppression of the AFM ordering temperature with increasing x. Inset: Phase diagram for $x=0.15$, showing the suppression of the paramagnetic to the AFQ transition temperature, as compared to pure CeB_6.

susceptibility occurs at very low applied magnetic field with decreasing temperature in the AFQ state that one would assume to retain the electric quadrapole ground state with decreasing temperature until the AFQ to antiferromagnetic (AFM) transition occurs. It appears that the ground state on individual Ce atoms is changing from electric quadrapole to magnetic dipole with decreasing temperature prior to the transition to the antiferromagnetic state.

Over the past ten years there have been many measurements of a partial phase diagram for trivalent La substitutions for Ce in CeB_6, see, for example, Ref. 9 for an example of studies covering a wide range of x. Most of the studies have been concerned with a narrow range of x extending from 0.6 to 0.75 to study the phase IV occurring in this range[10] and not at low concentrations to be compared with the current results on divalent doping. The few examples of low-concentration La in CeB_6 show that the phase II to phase III transition decreases with increasing amounts of La but not nearly as rapidly as is caused by the divalent doping.

In Fig. 6 the magnetization as a function of applied magnetic field comparing pure CeB_6 to the 10% sample shows

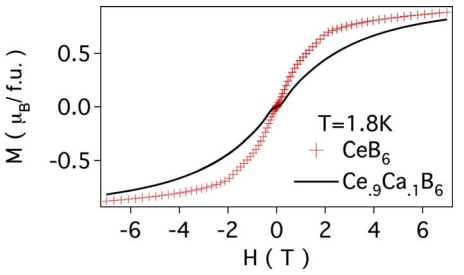

FIG. 6. (Color online) Magnetization per formula unit vs field in CeB_6 and $Ce_{0.95}Ca_{0.05}B_6$.

that the saturation magnetization is approaching the same magnetization as the pure CeB_6. Since there are fewer Ce atoms in the 5% sample, this could mean that a larger fraction of the total number of *f* electrons is localized than would be the case if the mixed-valence fraction remained the same between the two samples.

While decreases in FS size with divalent doping in trivalent compounds has been inferred previously due to changes from metal to insulator such as in Ca-doped GdB_6 (Ref. 11) no direct measurement of the FS volume of materials consisting of trivalent atoms as a function of divalent doping has been done in the past. We note that, as expected, no large change in the electronic properties in these three-dimensional, nonrelativistic electron FSs touching at a point occurs as in the case of two-dimensional relativistic electron-hole FS pockets touching at a point in graphene.[12] In conclusion, we find that divalent substitutions for trivalent La in LaB_6 decrease the volume of the FS in direct proportion to the decrease in the number of conduction electrons showing two overlapping pieces of FS becoming separated with decreased number of conduction electrons. The FS volume of divalent-doped CeB_6 decreases in size as divalent atoms replace trivalent Ce but the overall decrease is not directly proportional to the amount of divalent substitution due to the localization of the $4f$ electrons of the Ce atoms. In addition, the magnetic phase diagram showing the phase I (paramagnetic) to phase II (antiferroquadrupolar) then to phase III (antiferromagnetic) transitions decrease toward $T=0$ with increasing divalent substitution.

The work at the NHMFL was performed under the auspices of the National Science Foundation and the State of Florida. R.G.G. was supported directly by the NSF while Z.F. acknowledges Grant No. NSF-DMR-0503361 and D.P.Y. acknowledges Grant No. NSF-DMR-0449022.

*Present address: Department of Physics, George Washington University, Washington, DC 20052.

[1] R. G. Goodrich, N. Harrison, A. Teklu, D. Young, and Z. Fisk, Phys. Rev. Lett. **82**, 3669 (1999).

[2] A. P. J. Arko, G. Crabtree, D. Karim, F. M. Mueller, and L. R. Windmiller, Phys. Rev. B **13**, 5240 (1976); Y. Ishizawa, T. Tanaka, E. Bannai, and S. Kawai, J. Phys. Soc. Jpn. **42**, 112 (1977).

[3] R. G. Goodrich, N. Harrison, J. J. Vuillemin, A. Teklu, D. W. Hall, Z. Fisk, D. Young, and J. Sarrao, Phys. Rev. B **58**, 14896 (1998).

[4] A. A. Teklu, R. G. Goodrich, N. Harrison, D. Hall, Z. Fisk, and D. Young, Phys. Rev. B **62**, 12875 (2000).

[5] M. Kasaya, J. M. Tarascon, and J. Etourneau, Solid State Commun. **33**, 1005 (1980).

[6] C. H. Booth, J. L. Sarrao, M. F. Hundley, A. L. Cornelius, G. H. Kwei, A. Bianchi, Z. Fisk, and J. M. Lawrence, Phys. Rev. B **63**, 224302 (2001).

[7] N. Harrison, D. W. Hall, R. G. Goodrich, J. J. Vuillemin, and Z. Fisk, Phys. Rev. Lett. **81**, 870 (1998).

[8] E. G. Haanappel, R. Hedderich, W. Joss, S. Askenazy, and Z. Fisk, Physica B **177**, 181 (1992).

[9] M. Hiroi, S. Kobayashi, M. Sera, N. Kobayashi, and S. Kunii, J. Phys. Soc. Jpn. **67**, 53 (1998).

[10] T. Nagao and J. Igarashi, Phys. Rev. B, **74**, 104404 (2006); T. Morie, T. Sakakibara, T. Tayama, and S. Kunii, J. Phys. Soc. Jpn. **73**, 2381 (2004); S. Kobayashi, M. Sera, M. Hiroi, N. Kobayashi, and S. Kunii, Physica B **281-282**, 557 (2000).

[11] R. R. Urbano, P. G. Pagliuso, C. Rettori, P. Schlottmann, J. L. Sarrao, A. Bianchi, S. Nakatsuji, Z. Fisk, E. Velazquez, and S. B. Oseroff, Phys. Rev. B **71**, 184422 (2005).

[12] Y. Zhang, Y.-W. Tan, H. L. Stormer, and P. Kim, Nature (London) **438**, 201 (2005).